Chapter 10
Investigation of Control Signal Noise on an Acoustic Levitator Transducer Response

Wensheng Hu and Michael W. Sracic

Abstract This study investigates the coupling between broadband electronic noise and structural modal responses in an acoustic levitator transducer system. The transducer is nominally driven by a 27.75 kHz sinusoidal carrier, while controlled Gaussian band-limited noise is superimposed using an arbitrary waveform generator. The noise bandwidth is limited to 45 kHz via frequency-domain filtering, and its intensity is varied using RMS-based signal-to-noise ratio (SNR) control. Time-domain signals of acoustic pressure above the transducer radiating surface are acquired and analyzed in the frequency domain using FFT-based spectral estimation. Results reveal that increasing noise RMS does not significantly alter the primary operating peak near 27.75 kHz but leads to pronounced amplification of distinct low-frequency modal peaks, particularly around 10 kHz. To quantify this effect, the amplitude of the dominant low-frequency mode is normalized by the carrier peak amplitude, and the resulting ratio is evaluated as a function of SNR. A clear monotonic increase in normalized modal magnitude is observed as SNR decreases. These findings demonstrate that broadband electronic noise can activate off-operation-frequency structural resonances within high-frequency acoustic systems. The results highlight the importance of structural stiffness and electronic noise management in precision acoustic levitation platforms and provide experimental evidence of modal amplification under stochastic excitation.

Keywords Acoustic Levitator · Noise · Modal Excitation

Introduction

Acoustic levitation enables the containerless manipulation of materials by generating standing waves between an ultrasonic transducer and a reflector [1, 2]. With this configuration, stable levitation of an object may be achieved if the pressures in the field are large enough. However, many factors can lead to unstable levitation such as low pressure amplitudes, errors in system alignment, or nonlinear response of the transducer. For example, researchers have demonstrated that the transducer and reflector should be separated by a multiple of the standing wave's half wavelength [2, 3]. Deviations from this offset can reduce pressure amplitudes and overall levitation stability, which is critical for such applications as protein crystallography [1]. The transducers can respond nonlinearly which can also affect the stability of a levitated particle. This effect was shown by Feeney et al. [5], Aurelle et al. [6], and Alvarez et al. [7]. These errors of alignment or transducer response can be reduced with good design, and many successful levitation systems have been produced (e.g., [8, 9]).

Despite the theoretical maturity of these systems, practical setups must contend with non-ideal driving conditions. Modern levitators increasingly rely on complex signal synthesis and phased arrays to shape the sound field [4]. However, this complexity makes the system more vulnerable to electronic noise. Muelas-Hurtado and Contreras recently highlighted that these resonators are highly sensitive to internal reflections, meaning that even minor variations in the driving signal can lead to unexpectedly large fluctuations in the actual pressure amplitude [2]. While much research has focused on the precise

Wensheng Hu · Michael W. Sracic*
Mechanical Engineering Department, University of Wisconsin – Madison
503 Engineering Research Building, 1500 Engineering Drive, Madison, WI 53706 USA
e-mail: whu97@wisc.edu; mwsracic@wisc.edu

*Corresponding Author

© The Author(s), under exclusive license to River Publishers 2026

Paul Allison et al. (eds.), *Dynamic Behavior of Materials, Volume 1, 2026*, Conference Proceedings
of the Society for Experimental Mechanics Series, https://doi.org/10.13052/rp-9788743816249

design and optimization of these fields, the way random electronic noise interacts with the system's natural resonant modes is still not fully understood through experimental data.

In experimental practice, the impact of noise is often assessed indirectly by observing the motion of a levitated object [3]. Such metrics, however, fail to separate the noise in the electronic signal from the resulting physical response of the air gap. Direct spectral measurement is required to understand how electrical disturbances affect the transducer's response. For example, broadband electrical disturbances (i.e., "white noise") may excite unintentional frequencies of the transducer leading to nonlinear system response. In a system where the standing wave response of the airfield is reliant on a specific wavelength at steady state conditions, off-frequency disturbances introduce uncertainty into the precise control of the acoustic field and limit the reliability of the experimental results.

This study experimentally investigates how band-limited white noise in the control signal of an acoustic levitator affects the response of the transducer. Noise is injected into the control signal of a single-axis acoustic levitator. The response of the levitator transducer is measured with a high-frequency microphone placed near the transducer at multiple locations. The frequency spectrum of the pressure response is computed and used to characterize the resonant peaks. The objective is to quantify how the amplitudes of these specific resonant peaks are related to the amplitude of the noise in the control signal. The frequency spectra are compared to frequency response functions (FRFs) of the transducer that are also measured using the microphone. Finally, these resonant peaks from the noise corrupted response spectra are compared with FRFs to verify and validate those peaks as vibration modes of the transducer. This measurement-based approach provides a practical way to define the noise limits required for high-precision acoustic manipulation. The following sections of this paper provide the theoretical development, the methods, results and discussion, and the conclusions of the work.

Theoretical Development

Suppose a single-axis acoustic levitator has a transducer that is commanded with a sinusoidal control voltage

$$V(t) = Asin(\omega t) \tag{1}$$

where A is the voltage amplitude, $\omega = 2\pi f$ is the circular frequency for the operating frequency f. Under optimally designed conditions, the transducer will vibrate at the operating frequency f according to a linear transfer function theory. This is achieved by converting the electrical signal to a mechanical excitation using the piezoelectric effect. There are many works that document this effect and this theory is not the focus of this work. Here, we assume that the electrical control signal is converted to mechanical response with a transfer function, G, that depends on the electrical signal V.

$$x(t) = G(V, t) \tag{2}$$

If the system is linear, then the response x will contain a single frequency response with a magnitude that depends on the mechanical modes of the transducer. For example, in Clough et al. [8], the authors showed how the transducer should be operated near a specific resonance frequency of the transducer. However, the transducer is a continuous mechanical structure, and thus it has numerous resonance frequencies above and below the operating frequency. If any resonance frequency is excited besides the designed operating resonance frequency, a suboptimal system response may result. This would create uncertainty in the levitation airfield and instability in the levitated particle. In this work, we hypothesize that when bandlimited white noise of sufficient amplitude is added to Equation 1, multiple vibration modes may be excited in the transducer, and Equation 2 may represent a nonlinear transfer function in this case. In the next section, the Methods of the experimental work are described.

Experimental Platform

The experimental platform consisted of a single-axis acoustic levitator transducer. The transducer was designed with four Navy Type II piezoelectric discs, an aluminum endmass, and an aluminum horn. The transducer is mounted to a structural frame with aluminum brackets and clamps. This setup is shown and annotated in Figure 1.

The transducer was driven directly by a Siglent SDG1032X waveform generator at an operating frequency of 27.75 kHz. This operating frequency is known to excite a large vibration response of the transducer, which is capable of producing a standing wave with a reflector under the right conditions.

Preliminary measurements were conducted at multiple spatial locations across the radiating surface to ensure the consistency of the captured spectral signatures. Across all tested positions, the frequency sweep consistently exhibited identical

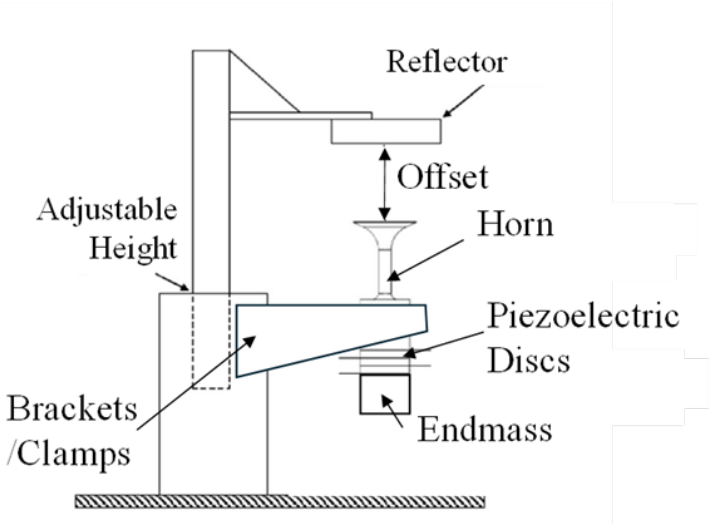

Fig. 1 Schematic of the Experimental Setup.

characteristic peaks and modal distributions, confirming that the observed response is a global property. To capture the acoustic response, a high-frequency microphone (PCB 378A14) was positioned near the radiating surface of the horn. This location was situated near the peripheral edge of the horn's centerline (Position 4 in Figure 2), rather than on the central acoustic axis. This is a location that is known to experience large amplitude vibrations at this operating frequency. The microphone position remained fixed throughout all experimental trials to ensure consistent measurement conditions. The measurement setup is shown in Figure 2. The microphone's output was conditioned and amplified using a PCB 480E09 ICP Sensor Signal Conditioner and was measured using a Keysight DSOX1204G oscilloscope. The following sections describe the baseline frequency response function acquisition as well as the system response when the control signal was corrupted with noise.

Baseline Frequency Sweep Measurement

Before introducing broadband noise to the control signal, a frequency sweep was performed to characterize the baseline response. The purpose of this measurement was to identify the natural modes of the system and to provide a reference for comparison with the noise-injection experiments. A sinusoidal frequency sweep ranging from 5,000 Hz to 30,000 Hz consisting of 250 measurement points was conducted using the built-in Frequency Response Analysis (FRA) of the Keysight DSOX1204G oscilloscope. At each frequency in the sweep, the generated sine function voltage and the microphone voltage were measured for several cycles of the steady state response. The amplitudes and relative phase of these signals were used to estimate the Frequency Response Function (FRF) of the Microphone Response (near the vibrating horn) relative to the control signal. During this test, no noise component was included. The resulting FRF is shown in Figure 4. The resulting curve showed multiple clear resonance peaks, which represent the natural modes.

Establishing this baseline is essential for the subsequent analysis. It allows for a clear distinction between the system's original properties and the responses observed after adding noise. Specifically, the band-limited noise introduced in the next stage does not create new frequencies. Instead, it provides a broadband energy source that activates these existing modes, allowing their development to be measured as the noise intensity increases.

Excitation Signal Design with Controlled Noise

The excitation signal was a composite waveform designed to investigate how the transducer's mechanical modes are excited by a noisy sine wave. The signal consisted of a deterministic 27.75 kHz sinusoidal wave superimposed with a stochastic noise component. While the sine wave was generated internally by the Siglent SDG1032X, the noise component was synthesized in MATLAB as an arbitrary waveform to ensure precise spectral control.

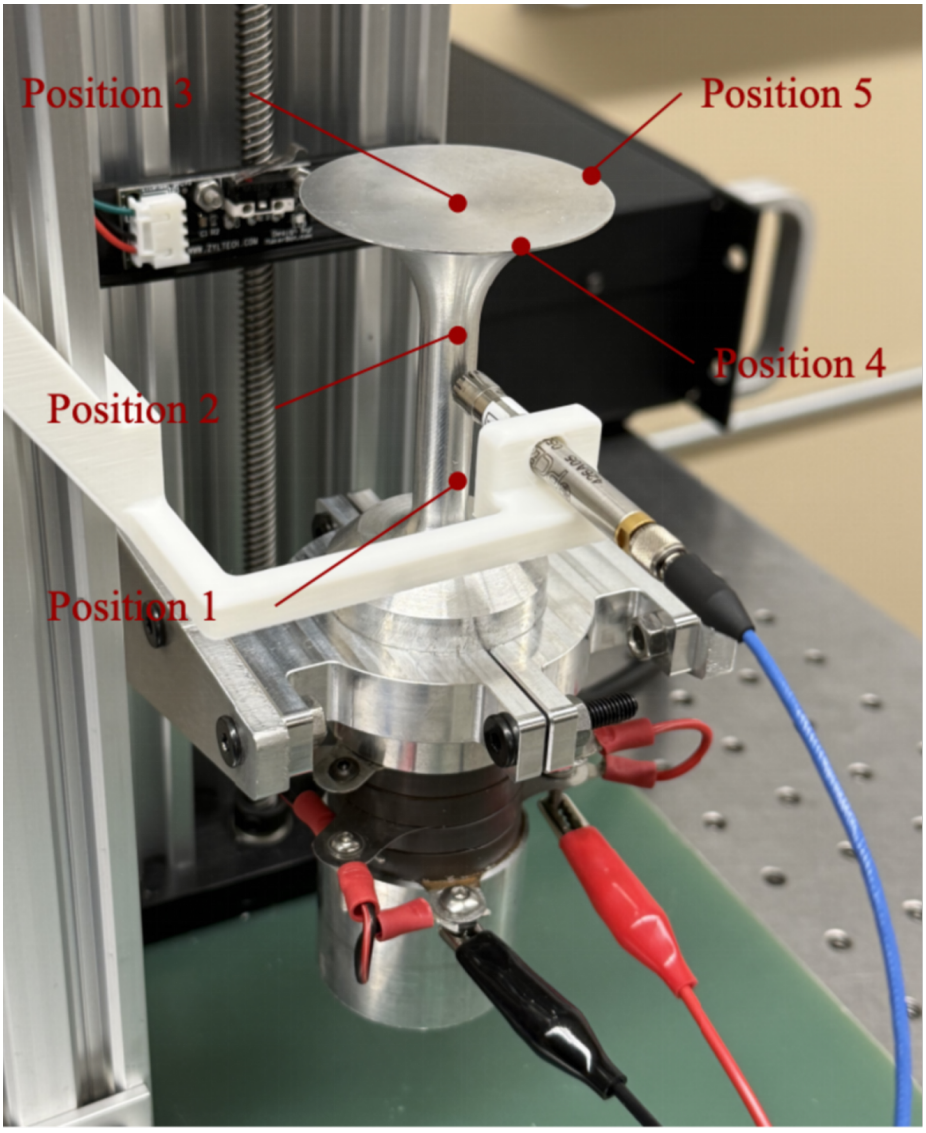

Fig. 2 Picture of Experimental Setup and measurement locations.

Specifically, the noise was generated as a Gaussian white sequence and processed using an FFT-based filtering method to set a cutoff frequency at 45 kHz. This frequency-domain approach was chosen to ensure seamless looping during hardware playback, preventing transient artifacts at the waveform boundaries. The filtered noise was normalized to a range of [-1,1] to utilize the full dynamic range of the waveform generator.

Throughout the experiments, signal amplitudes were characterized using root mean square (RMS) values to provide a consistent measure of effective excitation strength. The use of RMS values is particularly appropriate when defining the signal-to-noise ratio (SNR), since SNR is fundamentally a power-based metric. For electrical signals measured across a constant impedance, the average power is proportional to the square of the RMS voltage.

Accordingly, the signal-to-noise ratio in decibels is defined as

$$SNR_{dB} = 10log_{10}(\frac{P_{signal}}{P_{noise}}). \tag{3}$$

Substituting the power-voltage relationship yields

$$SNR_{dB} = 10log_{10}(\frac{{V^2}_{signal,\,RMS}}{{V^2}_{noise,\,RMS}}) = 20log_{10}(\frac{V_{signal,\,RMS}}{V_{noise,\,RMS}}). \tag{4}$$

The sinusoidal carrier amplitude was kept constant across all trials and was set to a peak-to-peak voltage of 5 volts. The RMS voltage of a sinusoidal wave can be written in terms of the peak-to-peak voltage as

$$V_{RMS} = \frac{V_{PP}}{2\sqrt{2}} \tag{5}$$

For the noise component, the normalized arbitrary waveform possessed a fixed RMS level prior to scaling. The actual noise RMS amplitude delivered to the system was then controlled by adjusting the peak-to-peak voltage setting of the noise channel on the waveform generator. Because the waveform was normalized, the output RMS value scaled proportionally with the selected peak-to-peak voltage, enabling repeatable and quantitative control of the noise intensity.

$$V_{RMS,\,actual} = \frac{V_{PP}}{2} V_{RMS,\,norm} \tag{6}$$

By maintaining a constant carrier amplitude while increasing the RMS level of the noise component, this configuration allowed for a controlled assessment of how increasing electronic disturbances excite discrete modal peaks within the acoustic resonator.

These two components were merged using the waveform generator's internal combining function.

Experimental Procedure and Parameter Sweep

To evaluate the influence of electronic noise on modal excitation, a structured parameter sweep was conducted by varying the noise amplitude while maintaining a constant deterministic carrier. The sinusoidal excitation at 27.75 kHz was fixed at 5 V peak-to-peak, corresponding to an RMS amplitude of approximately 1.77 V. This carrier level remained unchanged throughout all experimental trials.

The noise waveform, generated and normalized in MATLAB, possessed a fixed reference RMS value prior to hardware scaling. During experiments, the effective noise level delivered to the system was adjusted by modifying the peak-to-peak voltage of the arbitrary waveform channel on the signal generator. Because the waveform had been normalized, the output RMS amplitude scaled proportionally with the selected voltage setting, enabling precise and repeatable control of noise intensity.

The parameter sweep spanned a broad range of signal-to-noise ratios (SNR), beginning with the baseline condition and progressively increasing the noise amplitude to reach low-SNR regimes near unity. The SNR levels were selected in discrete steps, decreasing gradually from high-SNR conditions (tens of decibels) to low-SNR conditions approaching 1 dB. This incremental approach allowed for the identification of threshold behaviors and the progressive emergence of noise-induced modal excitation. An example time domain measurement of the voltage from the microphone above the horn is shown in Figure 3.

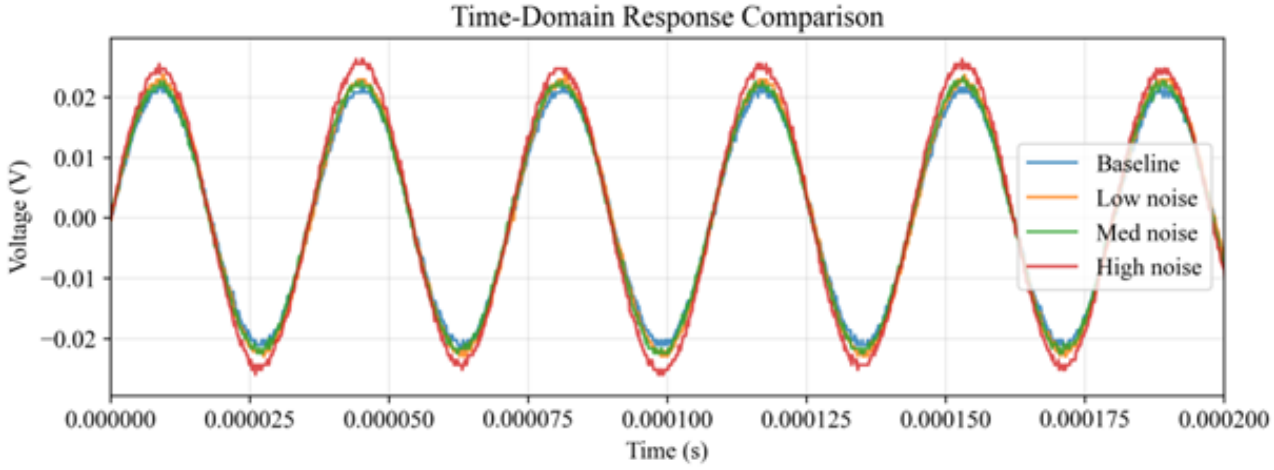

Fig. 3 Time-domain microphone output voltage representing the acoustic response for baseline and increasing noise levels.

Signal Processing and Spectral Analysis

To extract the frequency-domain characteristics of the transducer, the raw time-domain signals were processed using a customized spectral analysis pipeline implemented in Python. The objective was to obtain a stable, low-variance power spectrum that could clearly distinguish the system's modal peaks from the stochastic noise.

The processing was performed using Welch's method [10], which provides a more robust spectral estimate for random signals than a standard single-window FFT. First, the signals recorded at 100 MSa/s were divided into discrete segments. A Hanning window was applied to each segment to minimize spectral leakage and mitigate the effects of signal discontinuities at the sample boundaries. To ensure statistical reliability and improve the resolution of the spectral estimate, a 50% overlap was maintained between adjacent segments. For this study, a segment duration of 20 ms was utilized, providing a frequency resolution of approximately 50 Hz.

Following the windowing process, a Fast Fourier Transform (FFT) was performed on each segment, and the resulting periodograms were averaged in the frequency domain. This averaging process is essential for suppressing the random fluctuations inherent in the injected white noise. Finally, the spectral magnitudes were converted to a logarithmic scale (dB). Figure 5 shows the result of the frequency domain processing for the time domain signal in Figure 3.

To quantify the system's response across different trials, the amplitude of the identified low-frequency modes was normalized against the magnitude of the 27.75 kHz carrier signal. This standardized metric allows for a consistent comparison of modal activation as a function of the Signal-to-Noise Ratio (SNR).

Results and Discussion

Baseline Characterization via Frequency Sweep

The magnitude of the frequency response function of the transducer response at the horn is shown in Figure 4. Recall that this measurement was conducted in the absence of external noise. The spectrum reveals distinct peaks at several frequencies. The most prominent observation is a sharp gain peak centered at 27.75 kHz, confirming that the carrier signal is well-aligned with a strong vibration response at the horn surface. This alignment ensures that the large vibration of the horn is transferred to the air field of the levitator system. Another significant region of high response is observed at 10 kHz, and there are possible lower amplitude peaks at 19 kHz, 22 kHz, and 25 kHz.

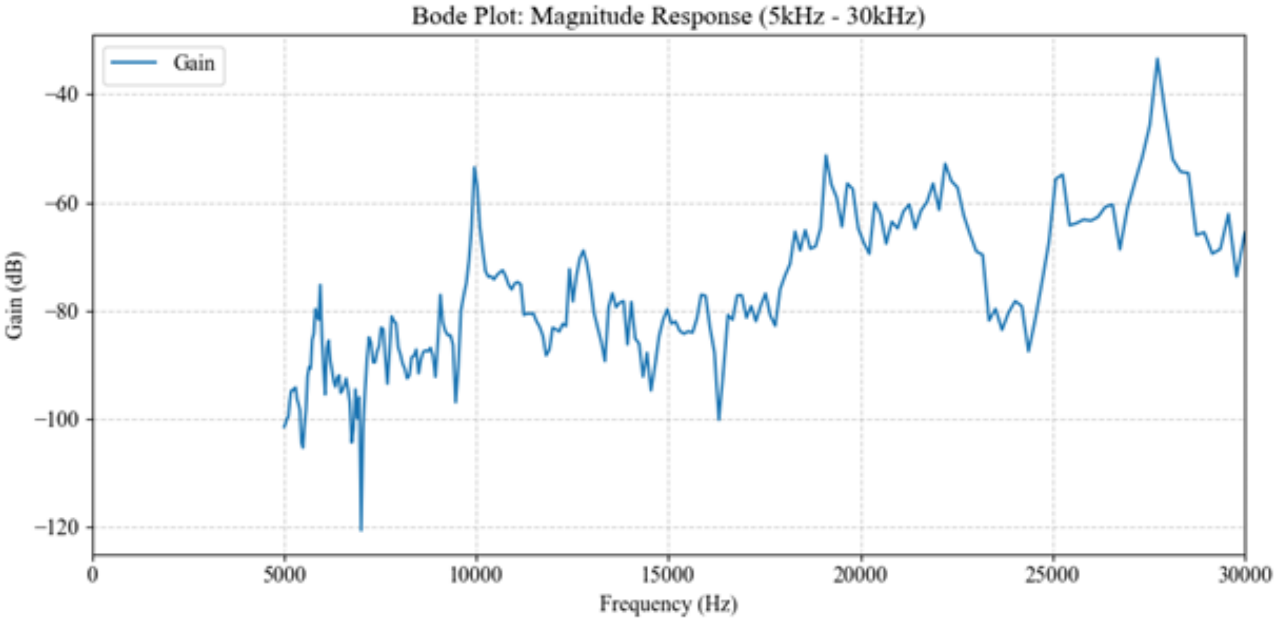

Fig. 4 Frequency Response Function Magnitude (Bode plot) of the acoustic transducer from 5 kHz to 30 kHz.

In typical mechanical design, one tends to avoid designing a system to operate near a resonance condition because large amplitude vibrations can lead to fatigue failures over time. For the acoustic levitator, the system is designed to operate at a single mechanical resonance to ensure large energy transfer from the transducer to the airfield. The design does not seek to excite any other modes as that would damage the airfield response and the target standing pressure wave. By establishing this baseline, we can confirm that any future peaks emerging at these specific frequencies during noise-injection trials are not random measurement artifacts, but a direct result of multi-modal activation.

Spectral Evolution Under Increasing Noise Levels

After the baseline FRF was measured, the control sinusoid was injected with noise and time domain measurements were taken and processed with the frequency domain method described previously. Noise levels labeled Baseline, Low noise, Med Noise, and High noise corresponding to SNR(dB) values of infinity, 30 dB, 15 dB, and 6 dB, respectively were measured. The magnitudes of the control spectral responses of the system are plotted from 0 to 30 kHz in Figure 5. The Baseline is shown with the blue curve, the Low noise is shown with the yellow curve, the Med Noise is shown with the green curve, and the High noise is shown with the red curve. Each of the curves shows a strong peak at the 27.75 kHz carrier signal. While the Baseline curve has no visible activity at lower frequencies, the other curves show a prominent peak at 10 kHz and the magnitude of that peak increases with the noise level. While this peak is barely detectable under Low noise conditions, it grows significantly as the noise level progresses to Med and High noise. There may also be a peaking response near 19 kHz and 22 kHz in the High noise response. Additionally, as broadband noise is injected, the noise floor across the entire band rises uniformly. This full-band comparison suggests that the cavity does not respond to noise in a purely uniform manner, but rather concentrates energy at specific spectral locations.

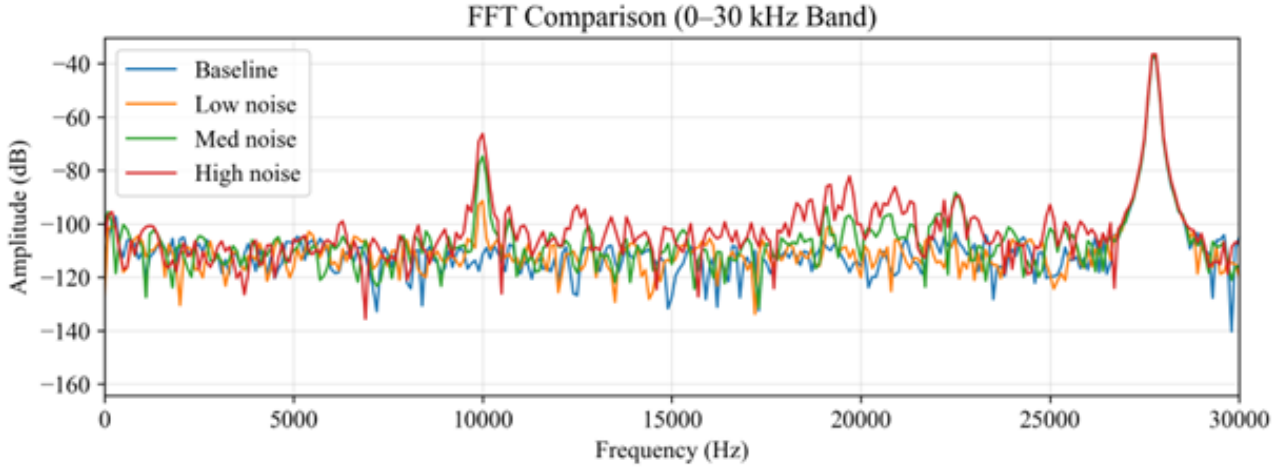

Fig. 5 Full-spectrum response from 0 to 30 kHz under varying noise excitation levels.

Detailed Spectral Analysis of Resonant Regions

To better analyze these spectral features, Figure 6 and Figure 7 provide magnified views of the critical frequency windows. Figure 6 focuses on the 10 kHz resonance, illustrating its steady growth with increasing noise level. This localized view confirms that the 10 kHz peak is the dominant structural response driven by external energy. Figure 7 examines the 15 to 30 kHz region, where subtle secondary fluctuations become visible only after the 10 kHz mode has reached a significant magnitude. These minor features suggest the sequential excitation of higher-order modes, though they remain substantially less pronounced than the primary resonance. The delayed and faint appearance of these fluctuations indicates that modal activation follows a hierarchical energy coupling process.

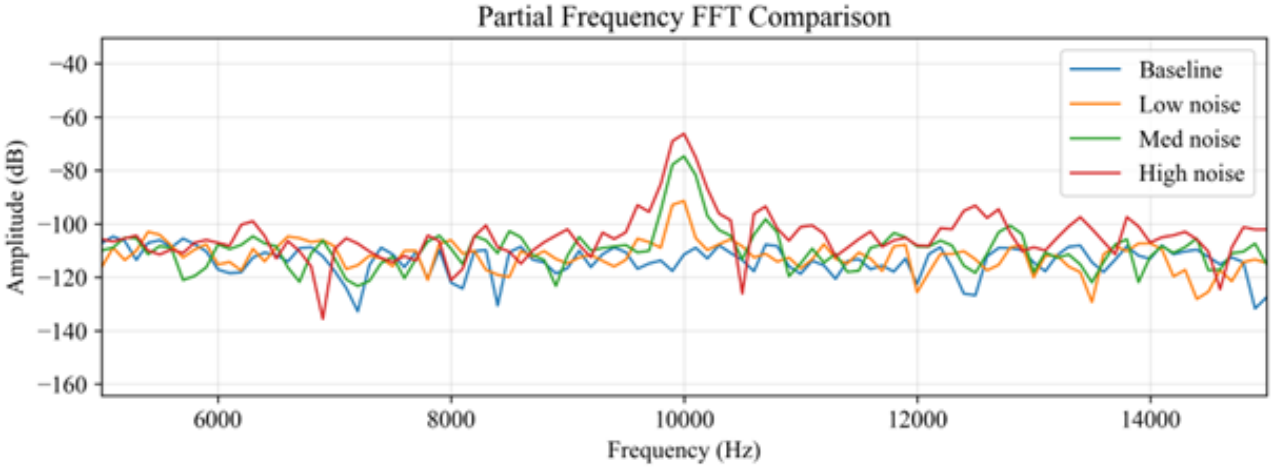

Fig. 6 Detailed spectral response near the 10 kHz resonant mode under varying noise levels.

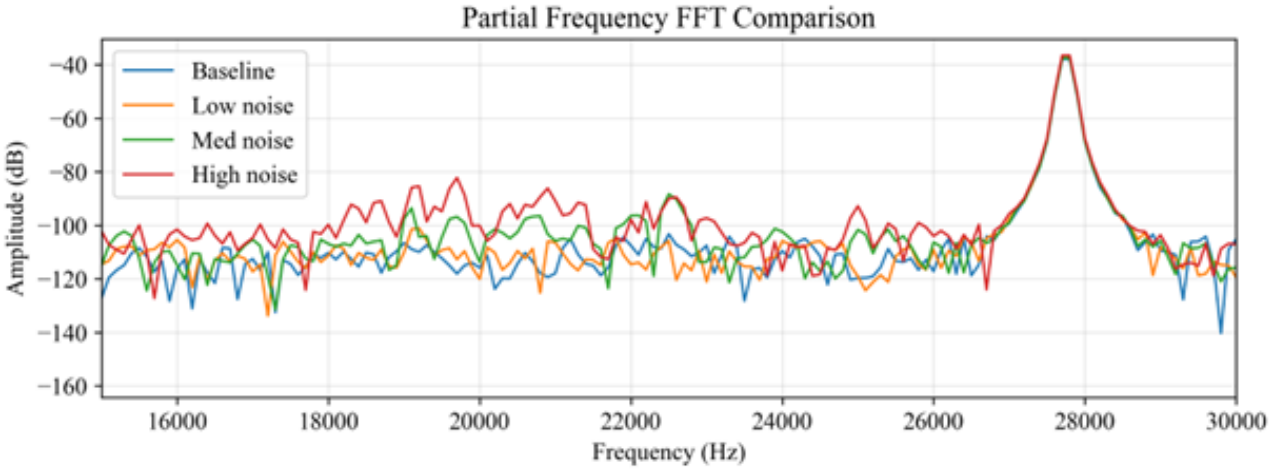

Fig. 7 Spectral response in the 15 kHz to 30 kHz range showing multiple secondary peaks preceding the operating frequency (27.75 kHz).

Quantitative Correlation Between Noise Level and Modal Response

To provide a quantitative measure of the observed phenomenon, the Normalized Magnitude (A_{mode}/A_{f0}) was calculated as a function of the Signal-to-Noise Ratio (SNR), as shown in Figure 8**.**

$$A_{normalized} = \frac{A_{mode}}{A_{f0}} \tag{7}$$

$$SNR_{dB} = 20log_{10}(\frac{A_{signal}}{A_{noise}}) \tag{8}$$

Within the 40 dB to 15 dB SNR range, the 10 kHz resonant mode exhibits a consistent upward trend. This suggests that the mode at 10 kHz is increasingly excited by energy from the increasing noise level. However, as the SNR drops below 10 dB, the curve displays increased fluctuations. It is important to note that the experimental range was constrained by the maximum output voltage of the generator. Consequently, these late-stage variations may represent experimental variance near the system's hardware limits rather than a definitive non-linearity. This trend validates that the 10 kHz mode can be activated by noise in the control signal with pronounced activation as the noise amplitude approaches the control sinusoidal amplitude.

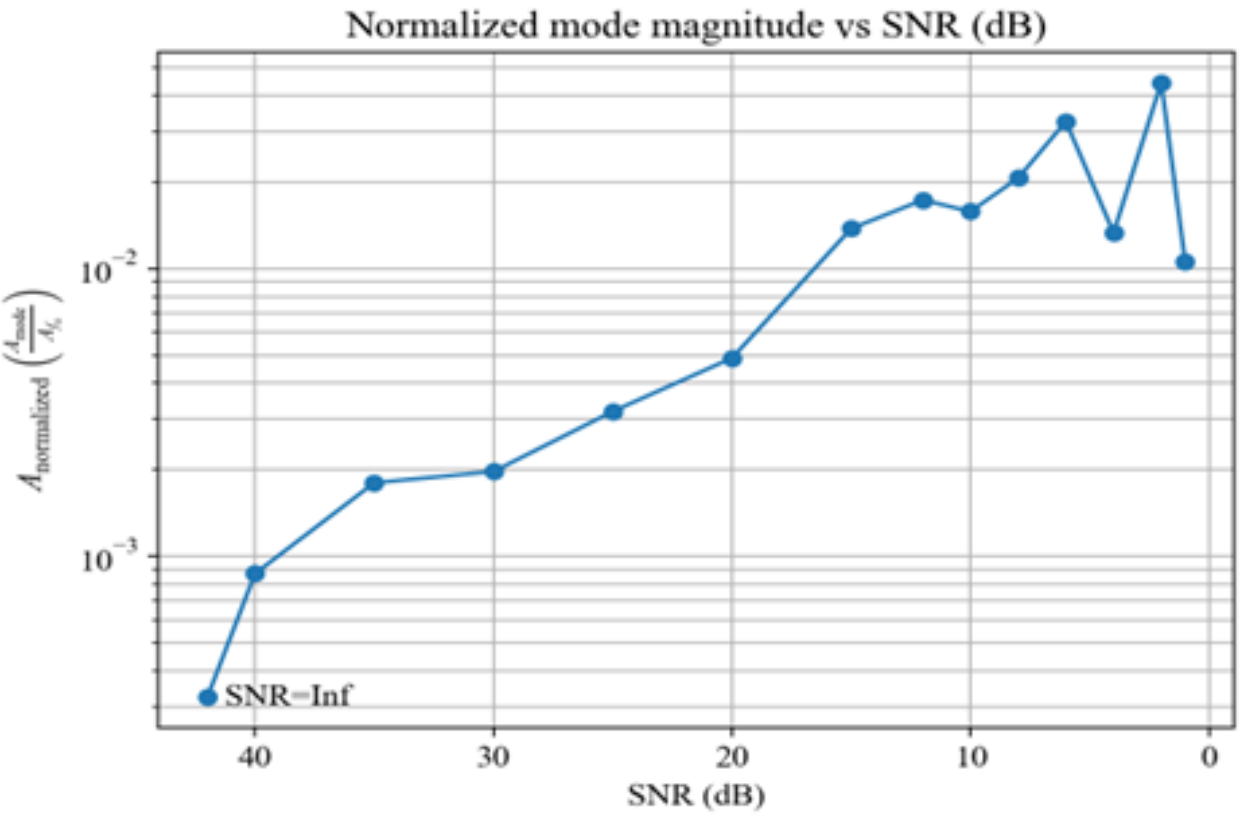

Fig. 8 Normalized magnitude of the 10 kHz acoustic mode as a function of the Signal-to-Noise Ratio (SNR).

Conclusion and Future Work

This study experimentally examined the influence of broadband electronic noise on the structural response of an acoustic levitation system operating at 27.75 kHz. By superimposing band-limited Gaussian noise onto a fixed sinusoidal carrier and systematically varying the signal-to-noise ratio (SNR), the frequency-domain behavior of the transducer's mechanical response was characterized using Welch-based spectral estimation.

The results show that increasing noise RMS does not significantly alter the primary operating peak but leads to pronounced amplification of discrete low-frequency structural modes, most notably near 10 kHz. When normalized by the carrier amplitude, the modal response exhibits a monotonic increase as SNR decreases, indicating energy-dependent excitation under stochastic forcing. These findings demonstrate that broadband electronic disturbances can activate intrinsic structural resonances even in systems designed for narrowband high-frequency operation.

Several experimental constraints should be acknowledged. The injected noise was implemented as a finite-length arbitrary waveform replayed cyclically by the waveform generator, resulting in a pseudo-random periodic realization rather than an ideal continuous stochastic process. In addition, the maximum achievable noise intensity was limited by the output voltage range of the signal generator, restricting exploration of lower SNR conditions. Furthermore, while the 10 kHz mode was consistently observable, other potential structural modes were less clearly distinguishable, possibly due to limited excitation energy or structural damping effects.

Despite these limitations, the observed modal amplification trend remains robust across tested SNR levels. Future work will focus on correlating the measured spectral peaks with finite element modal analysis and extending the excitation range to further investigate potential nonlinear coupling mechanisms.

Acknowledgments This work has been partially funded by Argonne National Laboratories through the University of Wisconsin's Mechanical Engineering Senior Design Program.

References

1. S. Tsujino and T. Tomizaki, “Ultrasonic acoustic levitation for fast frame rate X-ray protein crystallography at room temperature,” Scientific Reports, vol. 6, no. 1, p. 25558, 2016.
2. R. D. Muelas-Hurtado and V. Contreras, “The resonant behavior of airborne standing-wave acoustic levitators based on arrays of ultrasonic transducers,” Ultrasonics, vol. 145, p. 107454, 2025.
3. N. M. Brown, B. VanSaders, J. M. Kronenfeld, J. M. DeSimone, and H. M. Jaeger, “Direct measurement of forces in air-based acoustic levitation systems,” Review of Scientific Instruments, vol. 95, no. 9, 094901, 2024.
4. A. Marzo, S. A. Seah, B. W. Drinkwater, D. R. Sahoo, B. Long, and S. Subramanian, “Holographic acoustic elements for manipulation of levitated objects,” Nature Communications, vol. 6, no. 1, p. 8661, 2015.
5. A. Feeney, L. Kang, G. Rowlands, L. Zhou, S. Dixon, “Dynamic Nonlinearity in Piezoelectric Flexural Ultrasonic Transducers,” IEEE Sensors Journal, vol. 19, no. 15, p. 6056-6066, 2019.
6. N. Aurelle, D. Guyomar, C. Richard, P. Gonnard, and L. Eyraud, “Nonlinear behavior of an ultrasonic transducer,” Ultrasonics, vol. 34, p. 187-191, 1996.
7. N.P. Alvarez, A. Cardoni, N. Cerisola, E. Riera, M. Andrade, and J. Adamowski, “Nonlinear Dynamic Modeling of Langevin-Type Piezoelectric Transducers,” Actuators, vol. 4, p.255-266, 2015.
8. J. Clough, M. W. Sracic, D. Piombino, J. Braaten, S. Connors, N. Pedigo, V. Prantil, and K. Suthar, “Design and Prototype of a Two-Axis Acoustic Levitator,” Proceedings of the ASME 2016 International Mechanical Engineering Congress and Exposition, vol. 13, p. V013T01A002:1-10, 2016.
9. A. Marzo, A. Barnes, and B. W. Drinkwater, “TinyLev: A multi-emitter single-axis acoustic levitator,” Review of Scientific Instruments, vol. 88, no. 8, p. 085105, 2017.
10. P. Welch, “The use of fast Fourier transform for the estimation of power spectra: A method based on time averaging over short, modified periodograms,” IEEE Transactions on Audio and Electroacoustics, vol. 15, no. 2, p. 70-73, 1967.